

# FRACTAL ANALYSIS FOR HYPER-SPECTRUM IN REMOTE SENSING

Yamato YAMAURA, Susumu OGAWA  
Faculty of Geo-Environmental Science, Rissho University  
1700 Magechi, Kumagaya, Saitama 360-0194, JAPAN  
Phone: (81)-48-539-1652, Facsimile: (81)-48-539-1632  
E-mail: [031w00055@ris.ac.jp](mailto:031w00055@ris.ac.jp)

**KEYWORDS:** Aero-borne Remote Sensing, Agriculture, Land Covers, Semi-variograms

**ABSTRACT:** A hyper-spectrum in remote sensing has been used for identification of spectral information for land covers. First, a hyper-spectral image was overlapped the spatial map 25,000. Next, the spectra were extracted with hyper-spectral analysis. Finally, hyper-spectra were quantitatively evaluated by fractal analysis for each land cover. As a result, fractal analysis for hyper-spectrum in remote sensing was effective for identification of the spectral information for land covers.

## 1. INTRODUCTION

Crop growth and a land surface have been evaluated by the spectral information from a hyper-spectral image with aero-borne remote sensing. The spectra are described by the feature of a distribution with their patterns and intensities. Therefore, the main objective of this study was to evaluate land covers quantitatively with fractal analysis for hyper-spectrum in remote sensing.

## 2. STUDY AREA

A study area was Kumagaya city and Fukaya city, Saitama prefecture, Japan (Figure 1). These cities are located between the Tone River and the Arakawa River over the Shin-Arakawa alluvial fan. The soil is deep, fertile and appropriate for agriculture. In this study, the Menuma lowland, located between the Tone River and the Oyama River, which flow in the northern part of the city, was mainly researched.

**Table 1 Condition of the flight**

Area	Day/Month/Year	Fight Time
Kumagaya City	8/19/04	10:58
Fukaya City	2/28/04	11:24

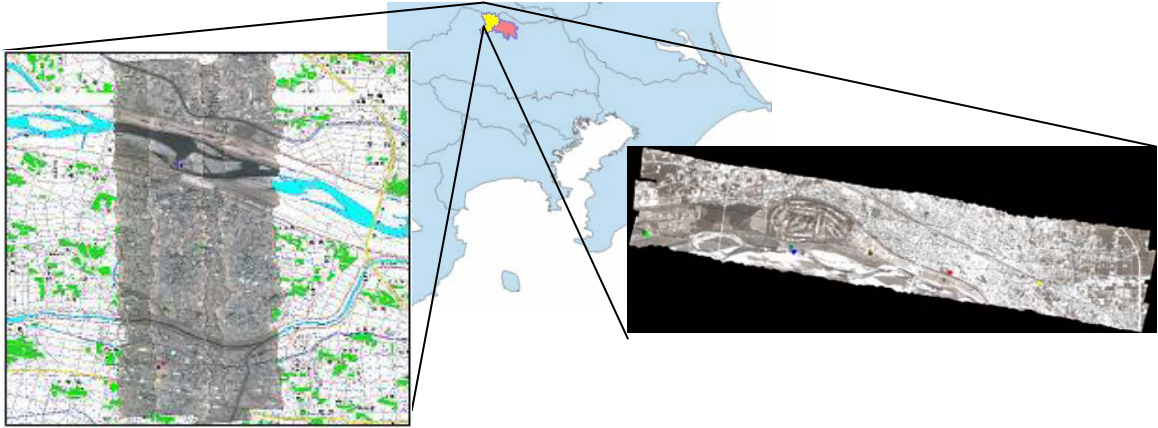


Figure 1 Hyper-spectral image in Kumagaya and Fukaya area

### 3. ANALYSIS METHOD

#### 3.1 Hyper-spectral Data in Remote Sensing

Hyper-spectral data have higher spectral resolution and more bands than traditional multi-spectral one. Hyper-spectral data analysis focuses on estimating the materials distributing in the study area from the feature of the profiles for spatially continuous spectra with high resolution. Here, the hyper-spectral data in aero-borne remote sensing are listed in the following Tables 3 to 8.

#### 3.2 Fractal Analysis for Spectra

Surface profiles of the earth and vegetation are recognized as self-similar shapes and fractal. In other words, a complex form of the nature is briefly characterized by a parameter, fractal dimension. In this study, fractal analysis was applied for hyper-spectra. For spectra of  $3 \times 3$  pixels in each land cover, fractal dimensions were obtained from semi-variograms as follows.

$$2\gamma(h) = E[Z_{x+h} - Z_x]^2 = h^{2H} \quad (1)$$

$$D = 2 - H \quad (2)$$

where  $\gamma(h)$ : the semi-variogram,  $E$ : expectation (variance),  $Z_{x+h}$ ,  $Z_x$ : the sampling amounts of  $x+h$  and  $x$ , respectively,  $h$ : a distance between two sampling points,  $H$ : the Hurst exponent. Assuming that variations of the sampling amounts are regressed by Equation (1),  $H$  is obtained

and  $D$  is calculated by Equation (2). Semi-variogram is referred to a *spatial variation* and is assumed to be fractal as a function of the distance.

## **4. ANALYSIS RESULTS**

### **4.1 Hyper-spectra in Each Land Cover**

Hyper-spectral results for each land cover were shown in Figures 5 to 10. The same spectral patterns were shown in both paddy fields and water body. Similarly, almost the same patterns were shown among broadleaf trees, conifer trees and crop fields. On the other hand, intense reflections and distinct variances of visible light were described in the road. However, either was clearly distinguished as to the spectral patterns. As shown in each figure, there were some significant differences in the reflection intensities for each land cover. It would be considered that they corresponded to the shapes of research objects and the physical properties.

### **4.2 Analysis Results**

Hyper spectral analysis for each land cover was conducted. Semi-variograms of each pixel were obtained; fractal dimensions were calculated by Equations (1) and (2). As shown in Table 2, there were some noticeable differences in fractal dimensions as well the reflection intensities. Those were derived from the shapes of research objects and the physical properties.

## **5. DISCUSSION**

The spectra for each land cover were evaluated quantitatively by fractal analysis for the hyper-spectral image. The differences in these hyper-spectral patterns were certainly noticeable, and could be classified by the fractal dimensions and the reflection intensities. Therefore, the properties of the research objects could be estimated. As a result, tree species, leaf areas and timber volumes might be informed from the hyper-spectral patterns of forest. Additionally, architectural structures, height and volumes might be also in the urban area.

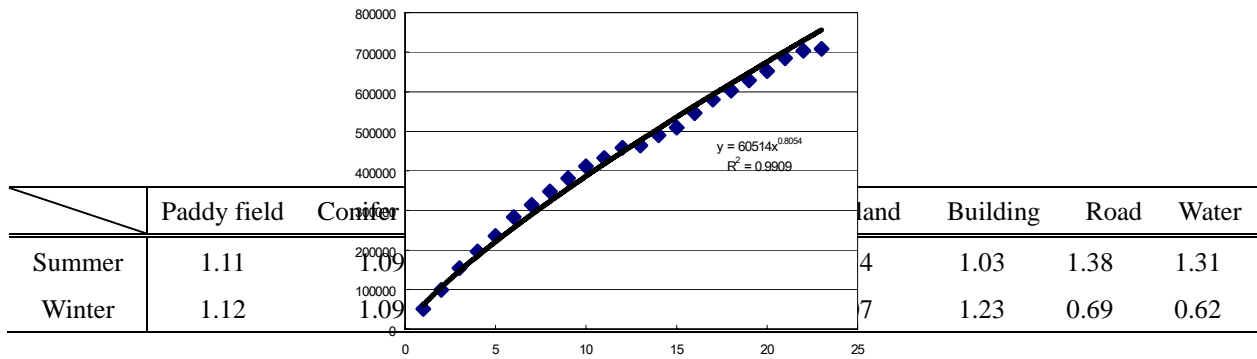
## **REFERENCES**

- [1] Ogawa, S., I. Makino, and G. Saito, 1999. Calculation of leaf area by fractal analysis for rice stubble structure, *Japan Society of Photogrammetry and Remote Sensing*, E-2 , pp. 73-76.
- [2] Ogawa, S., and T. Abe, 1994. Fractal evaluation on the spatial variation of pavement profiles, *Japan Society of Civil Engineers*, No.490/V-23 , pp. 131-136.
- [3] Ogawa, S., M. Hirano, T. Moriyama, and R. Ando, 1993. Fractal analysis of temporal and

spatial distributions for radar rain, *Committee on Hydro-science and Hydraulic Engineering*, No.37.

[4] Earth remote sensing data analysis center, 2005. Remote sensing for resource and environment in practical series 5. Use of Earth observation data (2).

[5] Takayasu, H., 1986. Fractal, Asakura Shoten.



[6] Hino, M., 1997. Fractal analysis, Asakura Shoten.

Semi-variogram

**Table 3 Specification of hyper-spectral sensor**

Hyper spectral sensor	AISA Concurrent
Output type	Unsigned 16bit
Spectral resolution	1.5m

**Table 4 Specification of hyper-spectral sensor**

Hyper spectral sensor	AISA Eagle
Output type	Unsigned 16bit
Spectral resolution	1.5m

**Figure 2 Semi-variogram**  
**Table 2 Pixel values in each land cover**

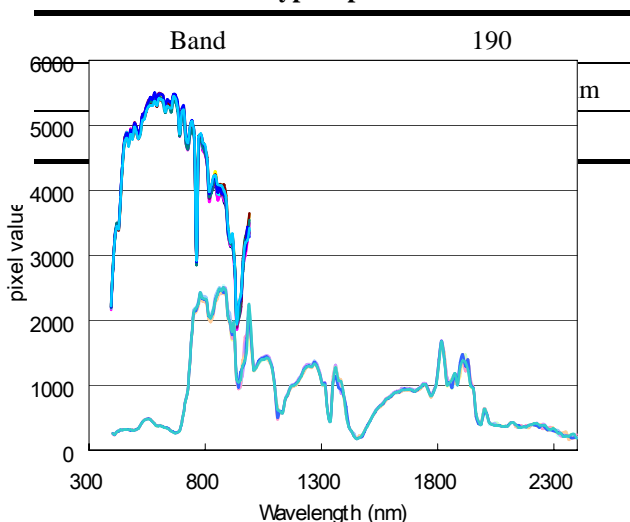
**Table 5 Projection drawing method**

Projection	UTM
Spheroid	WGS84
Datum	WGS84

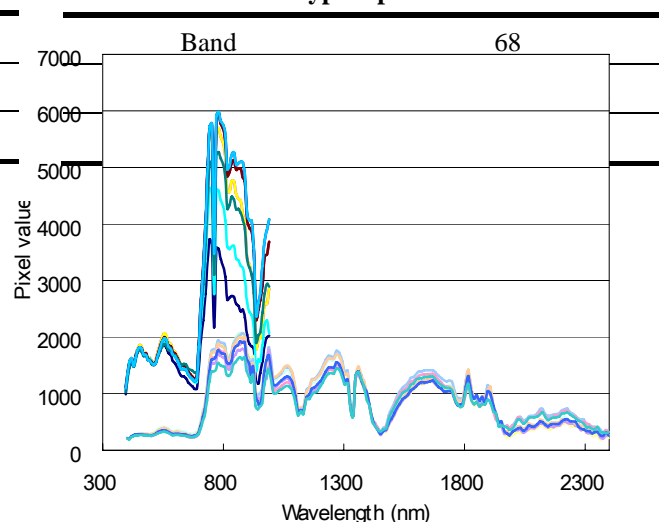
**Table 6 Projection drawing method**

Projection	Transverse Mercator
Spheroid	Bessel
Datum	Tokyo Japan

**Table 7 Hyper spectral data**



**Table 8 Hyper spectral data**



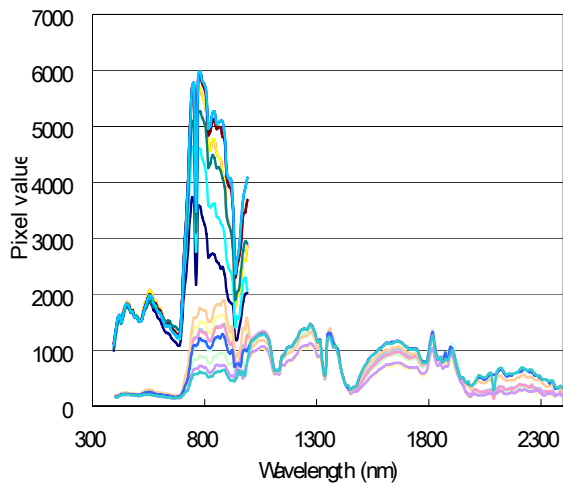


**Figure 5 Spectral profiles for broadleaf trees**

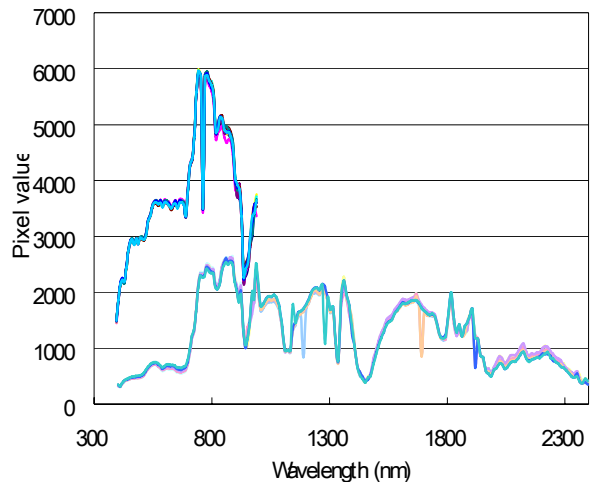


**Figure 6 Spectral profiles for crop fields**

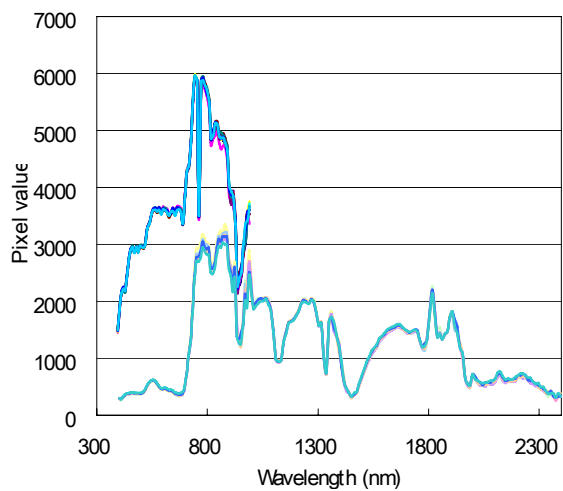


**Figure 7 Spectral profiles for buildings**

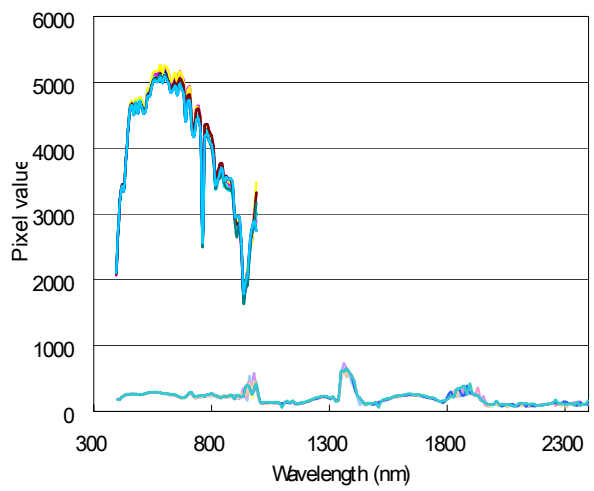


**Figure 8 Spectral profiles for water body**

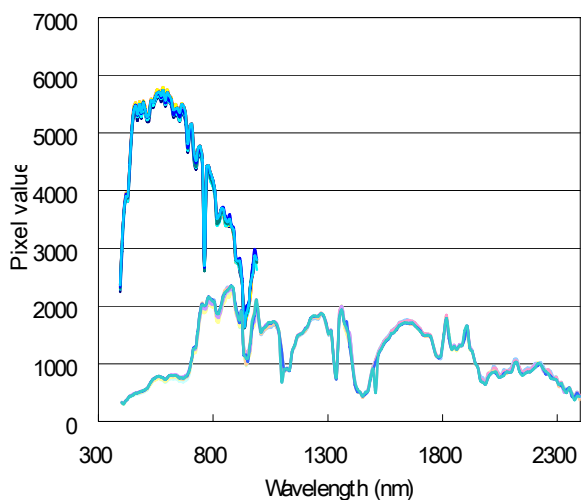


**Figure 9 Spectral profiles for bare lands**

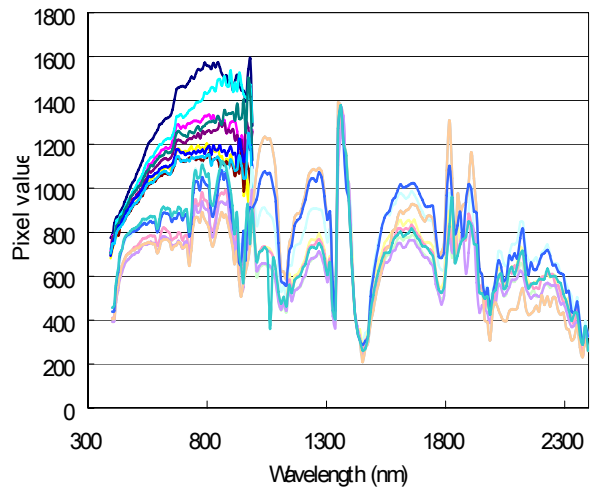


**Figure 10 Spectral profiles for roads**